



## **Modelling and analysis of a desiccant cooling system using the regenerative indirect evaporative cooling process**

**Bellemo, Lorenzo; Elmegaard, Brian; Reinholdt, Lars O.; Kærn, Martin Ryhl; Jakobsen, Arne; Markussen, Wiebke Brix**

*Published in:*

Proceedings of ECOS 2013 - The 26th International Conference on Efficiency, Cost, Optimization, Simulation and Environmental Impact of Energy Systems

*Publication date:*

2013

*Document Version*

Publisher's PDF, also known as Version of record

[Link back to DTU Orbit](#)

*Citation (APA):*

Bellemo, L., Elmegaard, B., Reinholdt, L. O., Kærn, M. R., Jakobsen, A., & Markussen, W. B. (2013). Modelling and analysis of a desiccant cooling system using the regenerative indirect evaporative cooling process. In *Proceedings of ECOS 2013 - The 26th International Conference on Efficiency, Cost, Optimization, Simulation and Environmental Impact of Energy Systems*

---

### **General rights**

Copyright and moral rights for the publications made accessible in the public portal are retained by the authors and/or other copyright owners and it is a condition of accessing publications that users recognise and abide by the legal requirements associated with these rights.

- Users may download and print one copy of any publication from the public portal for the purpose of private study or research.
- You may not further distribute the material or use it for any profit-making activity or commercial gain
- You may freely distribute the URL identifying the publication in the public portal

If you believe that this document breaches copyright please contact us providing details, and we will remove access to the work immediately and investigate your claim.

# Modelling and analysis of a desiccant cooling system using the regenerative indirect evaporative cooling process

*Lorenzo Bellemo<sup>a</sup>, Brian Elmegaard<sup>b</sup>, Lars O. Reinholdt<sup>c</sup>, Martin R. Kærn<sup>d</sup>, Arne Jakobsen<sup>e</sup>, Wiebke B. Markussen<sup>f</sup>*

<sup>a</sup> Technical University of Denmark DTU, Kongens Lyngby, Denmark, [lobel@mek.dtu.dk](mailto:lobel@mek.dtu.dk), CA

<sup>b</sup> Technical University of Denmark DTU, Kongens Lyngby, Denmark, [be@mek.dtu.dk](mailto:be@mek.dtu.dk)

<sup>c</sup> Danish Technological Institute DTI, Aarhus, Denmark, [lre@teknologisk.dk](mailto:lre@teknologisk.dk)

<sup>d</sup> Technical University of Denmark DTU, Kongens Lyngby, Denmark, [pmak@mek.dtu.dk](mailto:pmak@mek.dtu.dk)

<sup>d</sup> Technical University of Denmark DTU, Kongens Lyngby, Denmark, [arnja@mek.dtu.dk](mailto:arnja@mek.dtu.dk)

<sup>f</sup> Technical University of Denmark DTU, Kongens Lyngby, Denmark, [wb@mek.dtu.dk](mailto:wb@mek.dtu.dk)

## Abstract:

This paper focuses on the numerical modeling and analysis of a Desiccant Cooling (DEC) system with regenerative indirect evaporative cooling, termed Desiccant Dewpoint Cooling (DDC) system. The DDC system includes a Desiccant Wheel (DW), Dew Point Coolers (DPCs), a heat recovery unit and a heat source. Heat is used for dehumidification, whereas water is used for cooling and electricity for auxiliaries. An empirical DW model is built based on polynomial fits to manufacturer data. The DPC model is based on first principles, implementing heat and mass transfer using a 1D finite volume scheme and validated by manufacturer data. The models enable calculations of the steady state operation of the system. Alternative electric and absorption chiller-based systems are also modelled for benchmarking. The systems are simulated covering the internal loads of a specified supermarket during the summer period in different climates: temperate in Copenhagen and Mediterranean in Venice. Cheap and clean heat sources (e.g. solar energy) strongly increase the attractiveness of the DDC system. For the Mediterranean climate the DDC system represents a convenient alternative to chiller-based systems in terms of energy costs and CO<sub>2</sub> emissions. The electricity consumption for auxiliaries in the DDC system is higher than in the chiller-based systems. The number of commercial-size DPC units required to cover the cooling load during the whole period is high: 8 in Copenhagen and 12 in Venice.

## Keywords:

Desiccant, air conditioning, dehumidification, evaporative cooling, thermal energy.

## 1. Introduction

Security of supply and environmental impact largely affect the energy policies of many countries worldwide. In 2008 the EU adopted the so-called “20-20-20 by 2020” targets [1]: GHGs emissions and energy consumption have to be reduced, while increasing the share of renewables. All countries pursuing analogous targets have to apply significant changes to their energy systems, both by improving the efficiency of existing technologies and developing new ones.

The International Institute of Refrigeration in Paris estimated that the electricity consumption for refrigeration and air conditioning processes accounts for approximately 15% of the electricity production worldwide. In households and commercial buildings, air conditioning accounts for approximately 45% of the total energy consumption [2].

Air conditioning systems are designed to create and maintain indoor comfort by controlling thermo-hygrometric conditions, air quality and noise generation [3]. Nowadays the majority of these

systems are based on Vapour Compression Cycles (VCCs). VCCs and ab/adsorption chillers are cooling-based dehumidification technologies, i.e. they cool a surface in contact with humid air to cause condensation of moisture. A post-heating process is often needed to obtain the required supply temperature. The energy used to bring the air from the supply to the condensation temperature and back again represents an unavoidable energy surplus for all the cooling-based dehumidification technologies [4]: their efficiency drops for increasing latent loads.

## 1.1 – Desiccant cooling systems

Desiccant Cooling (DEC) systems are an alternative solution to cooling-based dehumidification technologies. DEC systems are generally characterized by three main components as presented in [4]: a desiccant dehumidifier, a cooling unit and a heat source. Therefore the latent and sensible loads are handled separately: the desiccant dehumidifier covers the latent load, while the cooling unit covers the sensible load.

Desiccants can be either solids or liquids. Their characteristics and fields of application are described in [5] and [6]. The dehumidifying mechanism of desiccants is sorption: an exothermic process during which the air in contact with the desiccant is simultaneously dried and heated, while the desiccant increases its water content being heated too. Usually liquid desiccants have higher sorption capacities, but solid desiccants allow compact designs with higher reliability, avoiding problems of corrosion. Regeneration of desiccants, i.e. moisture rejection, is achieved by heating the desiccant to sufficiently high temperatures: this is necessary to obtain a continuous dehumidification process. Low polluting and low grade heat sources, such as solar or waste heat, can be used for regeneration. In [2] it is reported that typical regeneration temperatures are around 65°C for liquid desiccants and adsorption chillers, 75°C for absorption chillers (LiBr/H<sub>2</sub>O), and 80°C for solid desiccants. The most common solid desiccant dehumidifier is the Desiccant Wheel (DW): several types of DEC systems using DWs are presented in [7].

The cooling load can be covered either by electricity (e.g. electric chillers), heat (e.g. absorption chillers), or water (e.g. evaporative coolers). In [8] it is demonstrated that cooling-based dehumidification technologies benefit from the integration with desiccant dehumidifiers because of increased evaporating temperatures. On the other hand, evaporative coolers benefit from dry air inlet conditions as discussed in [4]. Evaporative coolers can minimize the electricity consumption (electricity is always required for the auxiliaries) and avoid the use of harmful synthetic refrigerants in comparison to VCCs. A description of different types of evaporative coolers is reported in [9]. Indirect evaporative coolers do not increase the latent load on the desiccant dehumidifier since air is cooled at constant humidity ratio, differently from direct evaporative coolers. The Dew Point Cooler (DPC) is a regenerative indirect evaporative cooler that can theoretically cool down air to its dew point: evaporation takes place in a secondary airstream that is a recirculated fraction of the cooled primary airstream.

## 1.2 – Desiccant Dewpoint Cooling system

The Desiccant Dewpoint Cooling (DDC) system [10] is a specific DEC system, constituted by a Desiccant Wheel (DW) made of silica gel, a Heat Recovery Unit (HRU), a Dew Point Cooler (DPC), and a heat source connected to the system by means of a secondary hot water circuit. The heat source has to be chosen depending on the considered application (e.g. internal loads, geographical location, etc.). Several DPCs can be installed in parallel to cover high sensible loads. The resulting system is used for dehumidification, cooling and ventilation, while heating is not implemented in this study. The design of the DDC system is reported in Fig. 1 including fans, pumps, filters, and dampers that regulate recirculation from the conditioned space and bypass of the components.

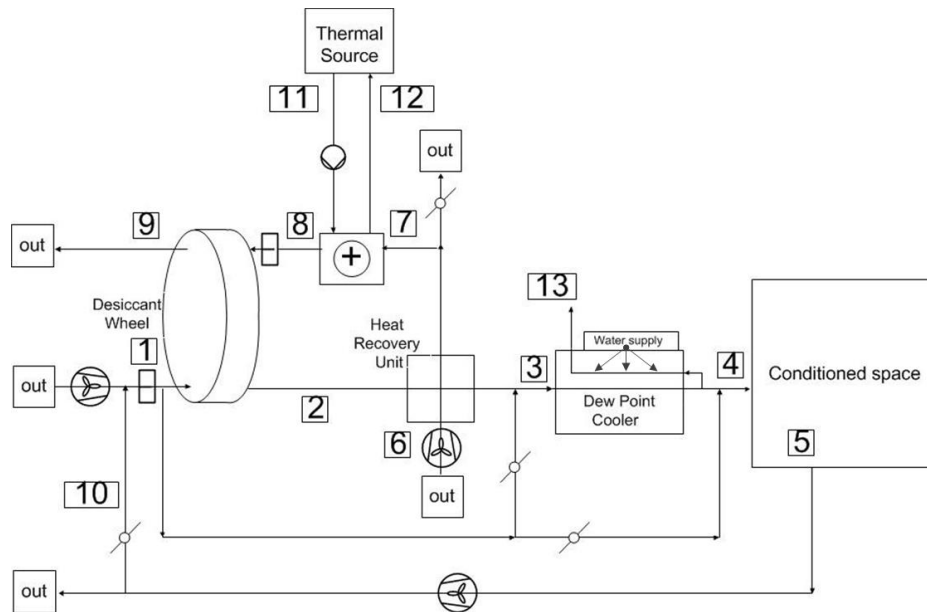


Fig. 1. DDC system design.

Similar DEC systems were proposed in [11] and [12]. The system optimization carried out in [12] highlighted that the electrical COP “*is the critical economic or environmental justification for installing a desiccant system*” when thermal sources such as solar or waste heat are available. However no direct comparison with other technologies was carried out.

The following analysis is meant to compare the DDC system performance to the performances of existing chiller-based systems (namely electric and absorption chillers). The comparison takes into account energy consumption, energy costs and CO<sub>2</sub> emissions. The systems are modelled and simulated for covering the sensible and latent loads in a specified supermarket during the summer period in two different climates.

### 1.3 – Case study

The DDC system is dimensioned to be used as centralized air conditioning unit for a specified supermarket, hence disregarding local load variations inside the building. Air conditioning systems for supermarkets are often designed to maintain the indoor relative humidity below a maximum value (e.g. 60-70%). Energy savings in the refrigeration system can be obtained by maintaining a low indoor relative humidity (e.g. 40%): less air condenses and freezes on the cold surfaces of refrigerated cases, decreasing both the thermal resistance on evaporators and the number of defrosting cycles. DEC systems decouple sensible and latent loads, allowing a better humidity control, and can recover the heat rejected from the refrigeration system.

The considered supermarket has an area of 750 m<sup>2</sup> and an internal sensible load of 37.5 kW. A Sensible Heat Ratio (ratio between sensible and total load) of 0.7 is assumed. The internal loads are assumed to be independent of the outdoor conditions in order to isolate the effect of different climatic conditions on the system performances. The indoor conditions are set to 23°C and relative humidity of 50%. The resulting air supply conditions from energy and mass balances correspond to 15.7°C and relative humidity of 68% at a flow rate of 15000 m<sup>3</sup>/h. These supply conditions are kept constant during the whole system operation because of the assumed constant internal loads.

## 2. Model formulation

The DDC system is modelled and implemented in Engineering Equation Solver (EES). Two alternative chiller-based systems are also modelled and implemented in EES. The models enable simulations of the steady state operation of the systems at the practical operating range, providing the consumptions of electricity, heat and water.

## 2.1. Desiccant Dewpoint Cooling system model

The DDC system design is reported in Fig. 1. Air from the environment (out) enters the system with the possibility of recirculation (10) of the exhausted air from the conditioned space (5) to lower the load on the system. Previous studies [13] on silica gel DWs demonstrated their high air cleaning potential, i.e. the supply air quality is good even with high shares of air exhausted from the conditioned space. The corresponding inlet air (1) is processed and supplied to the conditioned space (4). The process air is dehumidified (1-2), precooled in the HRU (2-3), and brought to the required supply temperature by means of the DPCs (3-4). A part of the cooled process airstream (4) is recirculated in the DPCs to provide the cooling effect. The recirculation fraction in the DPC is defined as the ratio between the secondary inlet and the primary outlet volume flow rates:

$$f_{rec} = \dot{V}_{s,in} / \dot{V}_{p,out} \quad (1)$$

The outgoing secondary airstream (13) is directly exhausted to the environment (out), not having any potential for sensible or latent heat recovery in the system.

The regeneration air is taken from the environment and preheated in the HRU (6-7). Differently from other DEC systems, the air recirculated from the conditioned space is not used for regeneration since already used for lowering the load on the system. The considered HRU is a balanced cross flow heat exchanger with a constant effectiveness of 0.7:

$$\varepsilon_{HRU} = \frac{T_7 - T_6}{T_2 - T_6} = \frac{T_2 - T_3}{T_2 - T_6} \quad (2)$$

The regeneration airflow (8) required in the DW to cover the latent load can be less than the process air flow rate (1). The ratio between the corresponding volume flow rates is termed regeneration fraction:

$$f_{reg} = \dot{V}_8 / \dot{V}_1 \quad (3)$$

The excess regeneration air is exhausted to the environment after the HRU. The net regeneration air is warmed up to the required regeneration temperature (8). The regeneration heat  $\dot{Q}_{reg}$  [kW] is calculated considering the air enthalpy difference  $\Delta I$  [kJ/kg<sub>a</sub>] at the regeneration heater:

$$\dot{Q}_{reg} = \dot{m}_{a,8} \cdot (I_8 - I_7) \quad (4)$$

After regeneration (8-9), the air is directly exhausted to the environment.

The system performance is assessed by means of both thermal and electric COPs, defined as:

$$COP_t = \frac{\dot{Q}_{load}}{\dot{Q}_{reg}} \quad (5)$$

$$COP_e = \frac{\dot{Q}_{load}}{\dot{W}_{aux}} \quad (6)$$

$\dot{Q}_{load}$  [kW] is the load covered by the system in the supermarket. We consider this quantity more meaningful than the air-side cooling capacity since the latter can turn negative when the process air requires dehumidification but not cooling: its enthalpy can be lower than the enthalpy at the supply conditions. This choice does not affect the validity of the comparison among different systems.

$\dot{W}_{aux}$  [kW] is the electric power consumption for auxiliaries. The electricity consumption of pumps and the electric motor moving the DW are negligible compared to the electricity consumption of fans, which is calculated as:

$$\dot{W}_{aux} = \frac{\dot{V}_a \cdot \Delta p}{\eta_{fan}} \quad (7)$$

$\eta_{fan}$  is assumed to be 50%, accounting for both the mechanical and electric efficiencies. An analogous value was used in [8] considering a brushless direct current motor. The pressure drops in

the system  $\Delta p$  [Pa] are either calculated (for DW and DPCs) or estimated (heat exchangers are assumed to cause a  $\Delta p$  of 100 Pa per side, while 80 Pa per filter).

### 2.1.1. Desiccant Wheel model

The DW is constituted by finely divided grains of desiccant material, impregnated onto a support structure: air flows through channels aligned lengthwise. The DW is divided in two sections: the process section, where adsorption takes place, and the regeneration section. The regeneration section is usually characterized by an angle between  $90^\circ$  and  $180^\circ$ . The DW rotates slowly, typically in the range 10-30 rph. An example of the DW functioning is reported in Fig. 2.

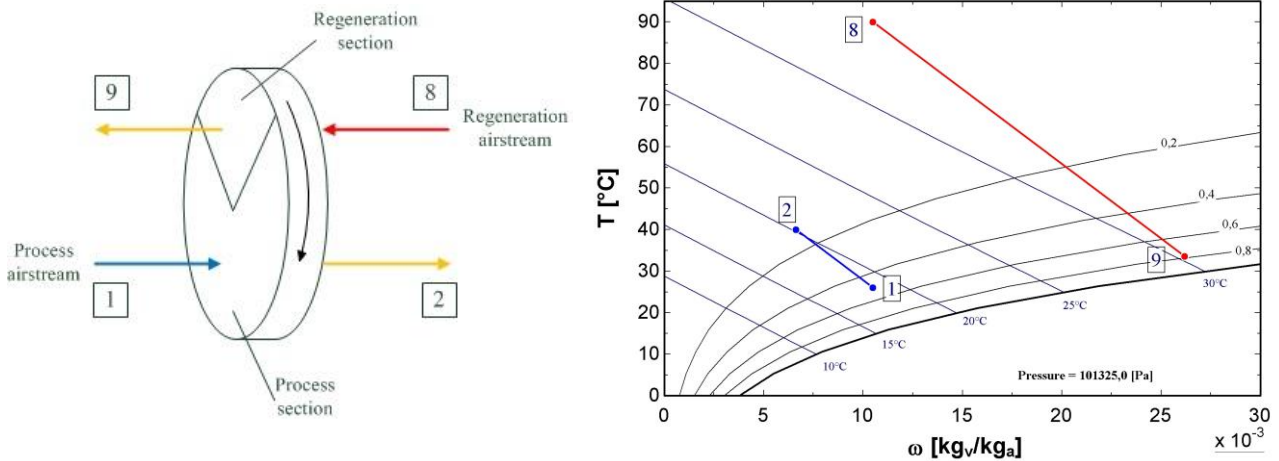


Fig. 2 Example of steady state operation of the DW with  $f_{reg}=0.3$ .

The process air is dehumidified and heated (1-2) increasing its enthalpy (adsorption). The regeneration air is humidified and cooled (8-9) decreasing its enthalpy (desorption).

Each desiccant has specific sorption characteristics depending on its level of saturation and humid air conditions. Temperature and moisture gradients generate both in the air and on the desiccant along the axial, radial and circumferential directions of the DW. A review of mathematical and empirical DW models is reported in [14].

In this study we develop empirical polynomial providing the process air outlet conditions ( $\omega_{p,out}$  and  $T_{p,out}$ ) and the pressure drops through both sections of the DW by fitting manufacturer data from *NovelAire* [15].

The parameters used to build the polynomials are the process air inlet temperature  $T_{p,in}$  and humidity ratio  $\omega_{p,in}$ , the regeneration air inlet temperature  $T_{reg}$  and humidity ratio  $\omega_{r,in}$ , and the process and regeneration air face velocities  $v_p$  and  $v_r$ . These parameters and the DW characteristics (desiccant material, dimensions, and rotational speed) determine the DW performance as described in [6].

The selected DW is made of silica gel, and it is dimensioned to process a range of airflow rates around  $22000 \text{ m}^3/\text{h}$ , which is required by the case study. The DW is characterized by a diameter of 1.73 m, a depth of 200 mm, and a regeneration angle of  $90^\circ$ . The manufacturer recommends a rotational speed of 24 rph. The minimum regeneration temperature  $T_{reg}$  is  $65^\circ\text{C}$ , while the minimum  $f_{reg}$  is in the range of 15-20% depending on  $T_{reg}$ .

Manufacturer data are gathered for all the combinations of parameters reported in Table 1,  $\omega_{r,in}$  is chosen to be equal to  $\omega_{p,in}$ .

Table 1. Considered values for the parameters characterising the DW performance

Parameters	Values
Process air volume flow rate $\dot{V}_{p,in}$ [m <sup>3</sup> /h]	20000 - 23000 - 26000
Regeneration fraction $f_{reg}$ [-]	0.2 - 0.4 - 0.6 - 0.8 - 1
Process air inlet temperature $T_{p,in}$ [°C]	15 - 20 - 25 - 30
Process air inlet relative humidity $\phi_{p,in}$ [%]	40 - 65 - 90
Regeneration temperature $T_{reg}$ [°C]	90 - 80 - 70

The polynomial structure for  $T_{p,out}$  and  $\omega_{p,out}$ , indicated with  $x$ , is:

$$x = c_{x1} \cdot v_p^{e_{x1}} + c_{x2} \cdot v_r^{e_{x2}} + c_{x3} \cdot T_{reg}^{e_{x3}} + c_{x4} \cdot T_{p,in}^{e_{x4}} + c_{x5} \cdot \omega_{p,in}^{e_{x5}} + c_{x6} \cdot \omega_{r,in}^{e_{x6}} \quad (8)$$

The polynomial structure for the process side pressure drop is:

$$\Delta p_p = c_{p0} + c_{p1} \cdot v_p^{e_{p1}} + c_{p2} \cdot T_{p,in}^{e_{p2}} + c_{p3} \cdot \omega_{p,in}^{e_{p3}} \quad (9)$$

The regeneration side pressure drop is calculated analogously.

The manufacturer data fitting is carried out by setting the exponents for each parameter, calculating the coefficients by means of a fitting function in MATLAB. The exponents are initially chosen from indications given in [6], and modified to minimize the Root Mean Square Error (RMSE) between the calculated outputs and the manufacturer data.

For the conditions reported in Table 1, the average RMSEs for  $T_{p,out}$  and  $\omega_{p,out}$  are  $\pm 1.1$  [°C] and  $\pm 0.3$  [g<sub>v</sub>/kg<sub>a</sub>] respectively. The estimated pressure drops have a maximum deviation of  $\pm 10\%$  from the manufacturer data.

The regeneration air outlet conditions are calculated applying energy and mass balances to the DW. The resulting adsorption and desorption processes are parallel on the Mollier diagram (Fig. 2).

### 2.1.2. Dew Point Cooler model

The considered DPC has a counter flow arrangement. The primary airstream is cooled into primary channels at a constant humidity ratio, and afterwards split into the secondary and the supply airstreams by a system of dampers. The secondary airstream is recirculated into secondary channels, where hygroscopic foils are spot-welded on the walls. Water is sprayed on top of the DPC, wetting the hygroscopic foils. The cooling effect is produced by the evaporation of water into the secondary airstream. The considered DPC has a nominal primary air flow rate of 4200 m<sup>3</sup>/h, with a maximum of 5600 m<sup>3</sup>/h. It is composed of 70 plates (i.e. primary channels) made of polypropylene, with a total height of 1.5 m and a length of 1.38 m. These characteristics refer to a DPC manufactured by *StatiqCooling* [16]. The DPC structure is shown in Fig. 3.

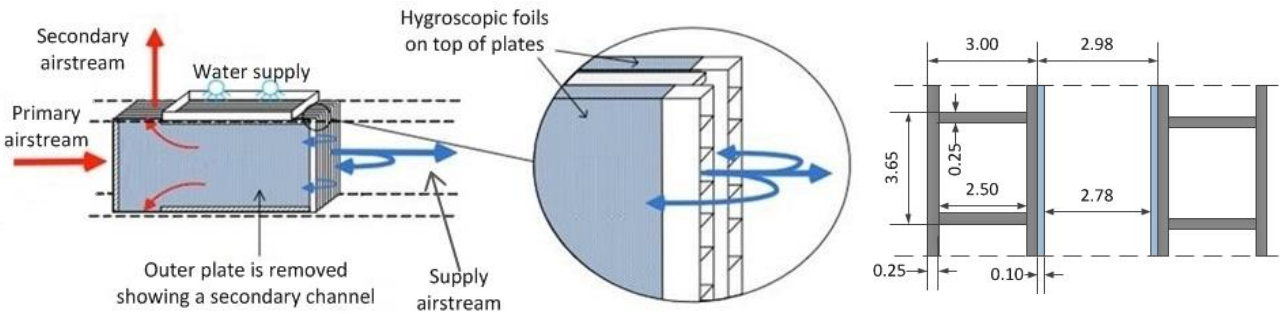


Fig. 3. DPC structure (external side view [17] and internal front view - dimensions in [mm])

The model is based on a 1D finite volume discretization along the DPC length. Heat and mass balances are applied and solved using the central difference scheme. The model is further described in Appendix A and [18]. A model of the same component was developed and presented in [17].

The resulting steady state working conditions are shown in Fig. 4. The primary airstream is cooled at a constant humidity ratio (1-2), while the secondary airstream is humidified and heated (3-4).

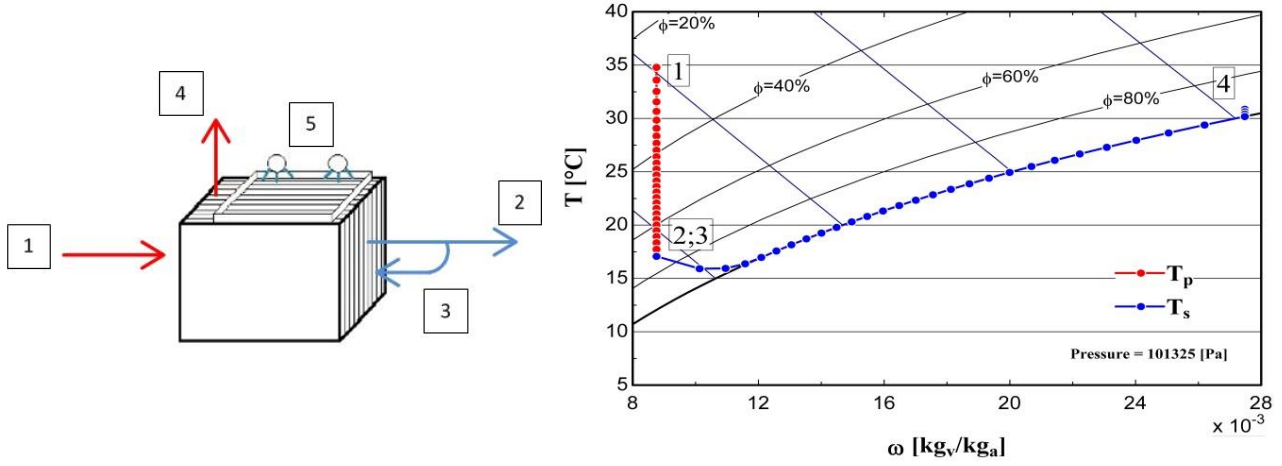


Fig. 4. Example of steady state operation of the DPC with  $f_{rec}=0.3$

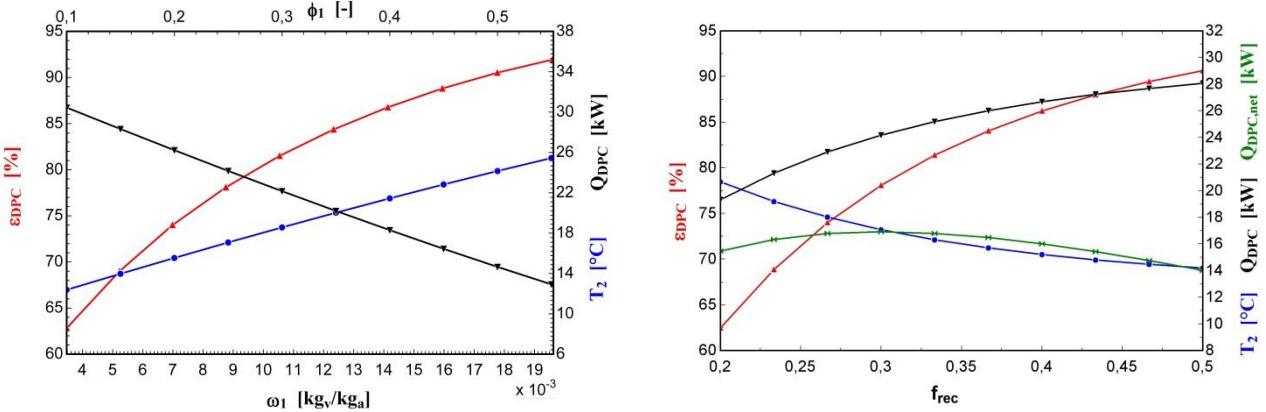
The DPC performance is estimated by means of the DPC (or dew point) effectiveness, cooling capacity and net cooling capacity. The cooling capacity takes into account the cooling provided to the primary airstream, while the net cooling capacity considers only the cooling provided to the supply airstream. Referring to the numbering used in Fig. , they are defined as:

$$\varepsilon_{DPC} = \frac{T_1 - T_2}{T_1 - T_{1,dp}} \quad (10)$$

$$\dot{Q}_{DPC} = \dot{m}_{a,1} \cdot (I_1 - I_2) = \dot{m}_{a,1} \cdot \bar{C}_p \cdot (T_1 - T_2) \quad (11)$$

$$\dot{Q}_{DPC,net} = (\dot{m}_{a,1} - \dot{m}_{a,3}) \cdot (I_1 - I_2) = \dot{m}_{a,1} \cdot \left(1 - f_{rec} \cdot \frac{\rho_3}{\rho_1}\right) \cdot \bar{C}_p \cdot (T_1 - T_2) \quad (12)$$

$T_{1,dp}$  is the dew point at the primary inlet conditions (1), i.e. the theoretical minimum temperature that may be reached. The supply temperature  $T_2$  varies with  $T_1$ ,  $\omega_1$ ,  $\dot{V}_1$ , and  $f_{rec}$ . From the model we observed that  $T_2$  is mostly affected by  $\omega_1$  and  $f_{rec}$ . Their influence on the DPC performance is shown in Fig. 5.



a)  $T_1=35^\circ\text{C}$ ,  $\dot{V}_1=4200 \text{ m}^3/\text{h}$ ,  $f_{rec}=0.3$

b)  $\dot{V}_1=4200 \text{ m}^3/\text{h}$ ,  $T_1=35^\circ\text{C}$ ,  $\Phi_1=25\%$

Fig. 5. DPC performance analysis.

Fig. 5a shows that  $T_2$  varies at a rate of  $0.8^\circ\text{C}/(\text{g}/\text{kg}_a)$  at the considered conditions. Varying  $T_1$  in the range  $20\text{-}45^\circ\text{C}$  ( $\dot{V}_1=4200 \text{ m}^3/\text{h}$ ,  $f_{rec}=0.3$ ,  $\omega_1=8 \text{ g}/\text{kg}_a$ ) makes  $T_2$  increase from  $14^\circ\text{C}$  to  $17^\circ\text{C}$ . Varying  $\dot{V}_1$  in the whole working range ( $1500\text{-}5600 \text{ m}^3/\text{h}$ ) makes  $T_2$  vary to a small extent. Fig. 5b shows that  $\dot{Q}_{DPC,net}$  is maximized for  $f_{rec}$  around 30%. Higher  $f_{rec}$  imply lower  $T_2$  but reduced supply flow rates.

The model is validated against manufacturer data. A result from the data fitting is shown in Table 2 for 6 representative steady state operating conditions. More than 20 different conditions were used

for validating the model. Table 2 shows the DPC performances from manufacturer data, the model under idealized conditions, and the tuned model to match manufacturer data.

Table 2. DPC model validation.

State	Manufacturer data			DPC model			Tuned DPC model		
	$\varepsilon_{DPC}$ [%]	$\dot{Q}_{DPC}$ [kW]	H <sub>2</sub> O [kg/h]	$\varepsilon_{DPC}$ [%]	$\dot{Q}_{DPC}$ [kW]	H <sub>2</sub> O [kg/h]	$\varepsilon_{DPC}$ [%]	$\dot{Q}_{DPC}$ [kW]	H <sub>2</sub> O [kg/h]
1	65	20.9	23.7	78	24.2	28.4	66	20.4	25.1
2	58	25.1	29.7	74	30.4	36.3	60	24.8	31.4
3	72	16.4	18.1	82	18.2	21.0	72	16.0	19.0
4	71	30.9	35.6	83	35.4	42.4	71	30.4	37.8
5	73	16.0	18.4	87	18.3	21.6	74	15.6	19.3
6	76	24.2	26.0	91	28.0	30.4	77	23.7	27.8

The model is tuned by setting a constant area effectiveness coefficient of 0.5 for all conditions, i.e. only half of the available area works at the conditions used to model the DPC. We propose that this difference is mainly due to inhomogeneous air and water distribution inside the DPC.

### 2.1.3. DDC system operation and control

Three operation profiles are defined for the DDC system:

- 1) The process air requires dehumidification. The system operates as shown in Fig. 6. The process air (blue line) is dehumidified and heated in the DW (1-2), precooled in the HRU (2-3), and cooled to the supply temperature in the DPCs at constant humidity ratio. The regeneration airstream (red line) is preheated in the HRU (out-7), heated to the regeneration temperature by the heat source (7-8), and used to regenerate the DW (8-9). Recirculation from the conditioned space (green line) is carried out by mixing outdoor air (out) and the whole exhaust air from the building (5,10). The process air after mixing (1) is constituted by approximately 68% of exhaust air and 32% of fresh air.  $\dot{Q}_{load}$  corresponds to 53.6 kW (sensible and latent loads).

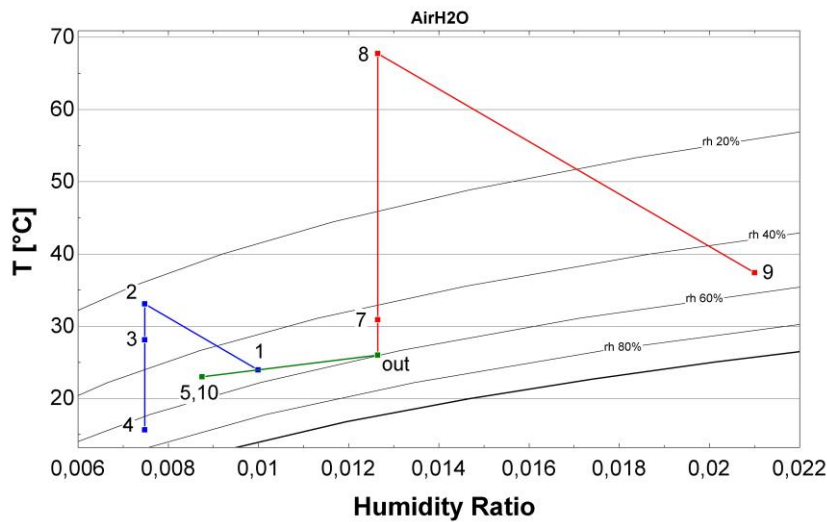


Fig. 6. Example of psychrometric processes in the DDC system operating with Profile1.

- 2) The process air requires only sensible cooling. The DW and HRU are bypassed and only the DPCs are active. The fan in the regeneration side is off.  $\dot{Q}_{load}$  corresponds to 37.5 kW (only sensible load).
- 3) The process air provides free cooling. Only ventilation is needed to guarantee a sufficient number of air changes per hour, while all components are bypassed. In case of particularly low outdoor temperatures it is be possible to add an additional heat exchanger connecting the heat source to the process air. This option is not investigated further in this study.  $\dot{Q}_{load}$  is null.

The DW operation is controlled by setting  $f_{reg}$  to 30%, while varying  $T_{reg}$  in the range 65-90°C to cover the required latent load at the air process side.  $f_{reg}$  can be varied in the range 20-30% keeping  $T_{reg}$  at 65°C and in the range 30-100% keeping  $T_{reg}$  at 90°C.

The DPCs are installed in parallel. More DPCs imply lower primary air flow rates per DPC, hence lower supply temperatures, and vice versa. A damper is installed in front of every DPC to regulate the primary air flow rate. We set  $f_{rec}$  constantly equal to 30%, providing the highest DPC net cooling capacity (see Fig. ) and not increasing the latent load on the DW (higher  $f_{reg}$  require to dehumidify higher air flow rates to obtain the same supply flow rates). Regulation of the water supply rate on top of the DPCs is not taken into account, being an output of the DPC model.

## 2.2. Chiller-based systems

Chiller-based systems are the common alternatives to the DDC system. We considered electric and absorption chillers. Their design and operation are shown in Fig. 7.

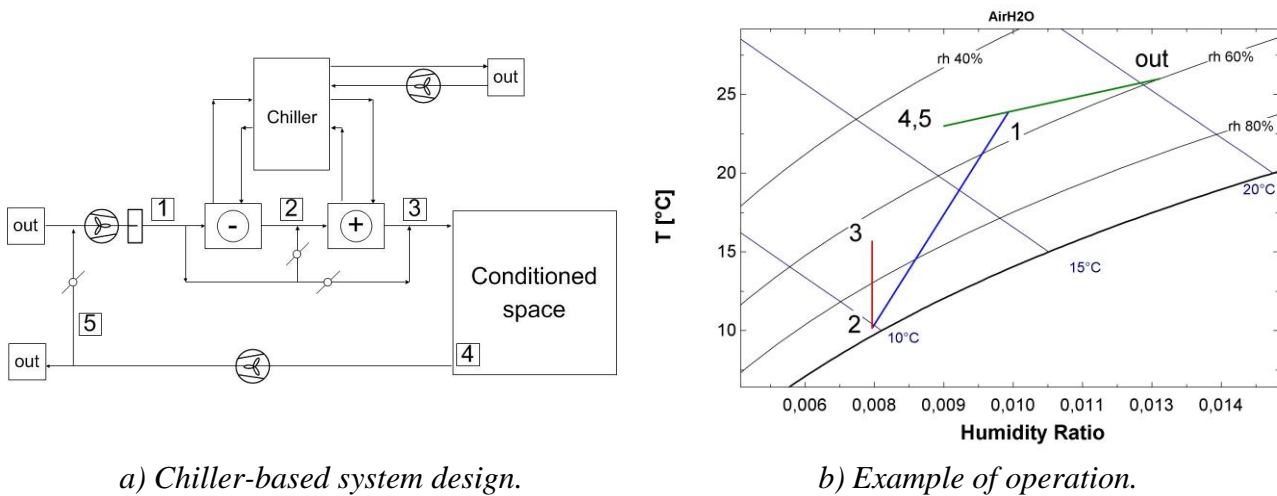


Fig. 7. Simplified design of chiller-based systems.

Recirculation is considered for the chiller-based systems too: the mixed process air (1) has the same composition of exhaust and fresh air as in the DDC system. Part of the heat rejected by the chillers is used for post heating. Operational profiles are defined analogously to the DDC system.

The COP of a chiller is defined as the ratio between the cooling load covered at the evaporator and the energy consumed: electricity for vapour compression in an electric chiller and heat for regeneration in an absorption chiller.

Two electric chillers are considered with constant COPs of 4.5 and 3.5 in order to cover a realistic range of performances. The correspondent systems are termed EC4.5 and EC3.5 respectively.

A LiBr/H<sub>2</sub>O absorption chiller is considered with constant COP of 0.71. In [19] it is reported that its COP at partial load does not vary significantly. The correspondent system is termed AC.

The electricity consumption for auxiliaries due to air circulation is calculated analogously to the DDC system. We assumed that 3% of the rejected heat is consumed as electricity for fans and pumps in the heat rejection circuits.

### 3. Results

The systems (DDC, EC4.5, EC3.5, AC) are simulated in two cities with different climates, namely Copenhagen and Venice. The simulations cover the period from May to September, on an hourly basis from 8 am to 9 pm every day. We assumed constant loads in the supermarket, hence constant supply conditions, to simplify the simulations and isolate the effect of varying climatic conditions on the system performances. Weather data are taken from the database contained in the software Pack Calculation II.

#### 3.1. Energy consumptions

Two recirculation control strategies are considered to lower the load on the systems: a Temperature Control (TC) and a Humidity Control (HC). With TC the exhaust air from the supermarket is recirculated when the indoor temperature is lower than the outdoor temperature. With HC the exhaust air is recirculated when the indoor humidity ratio is lower than the outdoor humidity ratio. The best recirculation control strategy is chosen comparing the energy performances of the DDC, EC4.5 and AC systems. The  $COP_{e,EC4.5}$  accounts only for the electricity consumed by the compressor. The results are reported in Table 3 and Table 4.

*Table 3. Energy performances of the systems in Copenhagen comparing TC and HC*

Period	$Q_{load}$ [MWh]	$COP_{t,DDC}$		$COP_{e,EC4.5}$		$COP_{t,AC}$	
		TC	HC	TC	HC	TC	HC
May	3.16	5.13	5.13	19.51	19.40	3.08	3.06
June	12.82	1.71	1.71	6.89	6.36	1.10	1.00
July	18.40	1.20	1.24	4.94	4.54	0.78	0.72
August	21.03	0.77	0.87	3.59	3.43	0.57	0.54
September	9.52	1.18	1.16	8.59	7.27	1.36	1.15
Seasonal	64.93	1.10	1.17	5.11	4.75	0.81	0.75

In Copenhagen the DDC system performs better with HC, while the chiller-based systems perform better with TC. The DDC system presents the biggest difference in August where its  $COP_t$  drops, i.e. the highest amount of regeneration energy is consumed. With TC the required regeneration power has a peak around 180 kW, dropping to 90 kW with HC. This may be due to the fact that sensible and latent loads have peaks at different hours during the day.

*Table 4. Energy performances of the systems in Venice comparing TC and HC*

Period	$Q_{load}$ [MWh]	$COP_{t,DDC}$		$COP_{e,EC4.5}$		$COP_{t,AC}$	
		TC	HC	TC	HC	TC	HC
May	19.49	0.83	0.98	3.38	3.43	0.53	0.54
June	20.02	0.67	0.78	2.61	2.72	0.41	0.43
July	21.44	0.51	0.57	2.17	2.23	0.34	0.35
August	21.59	0.55	0.63	2.27	2.37	0.36	0.37
September	19.53	0.73	0.90	3.03	3.23	0.48	0.51
Seasonal	102.07	0.63	0.74	2.60	2.70	0.41	0.42

In Venice all the systems perform better with HC. July is the most humid month implying the lowest COPs: with TC the regeneration power in the DDC system has a peak at 380 kW, dropping to 230 kW with HC. HC is always beneficial for the DDC system since the reduced load on the dehumidifier lowers the regeneration energy consumption.

We chose HC for all the systems, in order to reduce the regeneration energy consumption.

The  $COP_e$  of all the systems are reported in Table 5 and Table 6, taking into account also the electricity for the auxiliaries, together with the water consumption in the DDC system.

Table 5. Water consumption and electric COPs of the systems using HC in Copenhagen

Period	$V_{H_2O,DDC}$ [m <sup>3</sup> ]	$COP_{e,DDC}$	$COP_{e,EC4.5}$	$COP_{e,EC3.5}$	$COP_{e,AC}$
May	3.18	4.86	8.67	7.67	13.89
June	10.59	5.88	4.42	3.67	10.62
July	17.95	4.95	3.40	2.79	9.21
August	22.37	4.19	2.71	2.20	8.02
September	7.41	6.22	5.16	4.27	12.80
Seasonal	61.50	4.96	3.55	2.91	9.55

The minimum number of DPCs to cool down the whole process air flow rate is 4, corresponding to a primary air volume flow rate per DPC of approximately 5500 m<sup>3</sup>/h. In Copenhagen 8 DPCs have to be installed to always cover the cooling load: the primary air volume flow rate per DPC decreases to approximately 2750 m<sup>3</sup>/h. All these DPCs are required only for few hours in July and August. The AC has the highest  $COP_e$ , due to the electricity consumption of its auxiliaries. The consumptions of the auxiliaries in the ECs are lower than in the AC because of lower amounts of heat rejected: the AC has to reject heat from both the condenser and the absorber. Including the auxiliaries, the seasonal  $COP_{e,EC4.5}$  drops of 25%, from 4.75 (Table 3) to 3.55 (Table 5), while the seasonal  $COP_{e,EC3.5}$  drops of 21%. The DDC system has the highest electricity consumption for the auxiliaries.

Table 6. Water consumption and electric COPs of the systems using HC in Venice

Period	$V_{H_2O,DDC}$ [m <sup>3</sup> ]	$COP_{e,DDC}$	$COP_{e,EC4.5}$	$COP_{e,EC3.5}$	$COP_{e,AC}$
May	21.65	5.01	2.68	2.18	7.74
June	32.36	5.66	2.18	1.76	6.68
July	45.09	5.35	1.82	1.46	5.71
August	40.27	4.74	1.92	1.55	6.00
September	24.54	4.91	2.55	2.07	7.53
Seasonal	163.91	5.11	2.16	1.75	6.60

In Venice 12 DPCs are required, corresponding to a primary air volume flow rate per DPC of approximately 1850 m<sup>3</sup>/h.  $COP_{e,AC}$  is again the highest, but the difference with  $COP_{e,DDC}$  is reduced in comparison to Copenhagen. This is due to the higher dehumidification capacity required, which increases the amount of heat rejected from the AC. The seasonal  $COP_{e,EC4.5}$  drops of 20 % from 2.70 (Table 4) to 2.16 (Table 6), while the seasonal  $COP_{e,EC3.5}$  drops of 17%.

### 3.2. Energy costs

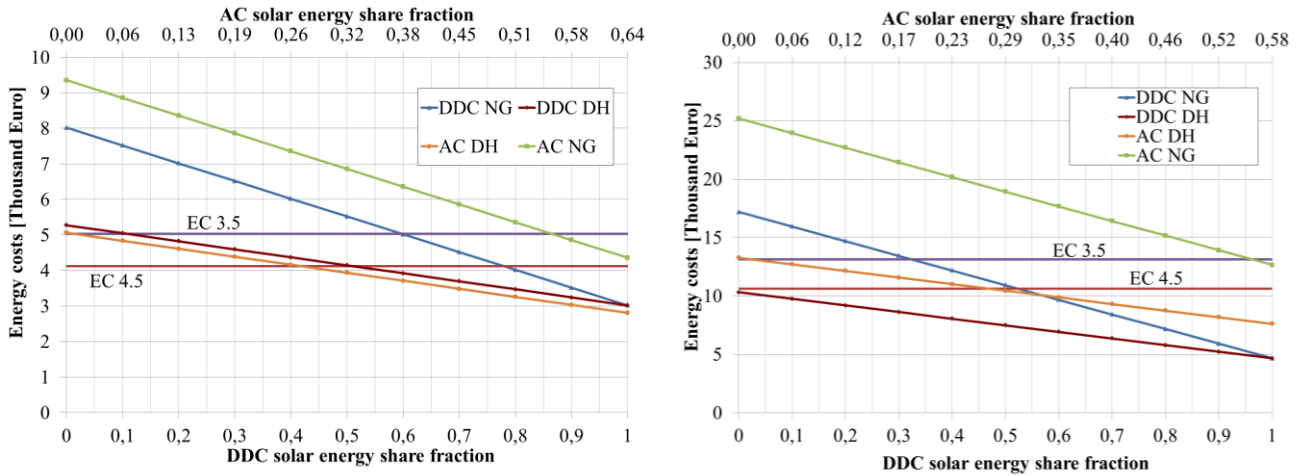
Two conventional heat sources are considered to feed both the DDC system and the AC: a boiler ( $\eta_{th}=95\%$ ) running on Natural Gas (NG) and District Heating (DH). The energy prices refer to the Danish scenario for the commercial sector (VAT not included): electricity 225 Euro/MWh, deionization of water 1.07 Euro/m<sup>3</sup><sub>H<sub>2</sub>O</sub>, NG 86 Euro/MWh<sub>fuel</sub>, and DH 41 Euro/MWh.

Solar energy is considered to cover a fraction of the regeneration loads of both the DDC system and the AC. The solar energy share fraction is defined as:

$$f_{solar} = \frac{Q_{solar}}{Q_{reg}} \quad (13)$$

Where  $Q_{solar}$  is the amount of heat from the solar heating system that is provided to the regeneration air (7-8 in Fig. 1). No hot water storage is considered as well as the electricity consumption for auxiliaries in both the solar heating system and boiler.

The DDC system always consumes less regeneration energy than the AC, therefore  $f_{solar,DDC}$  is varied between 0 and 1 and  $f_{solar,AC}$  is calculated for the corresponding  $Q_{solar}$ . The resulting energy costs for varying  $f_{solar}$  are reported in Fig. 8.



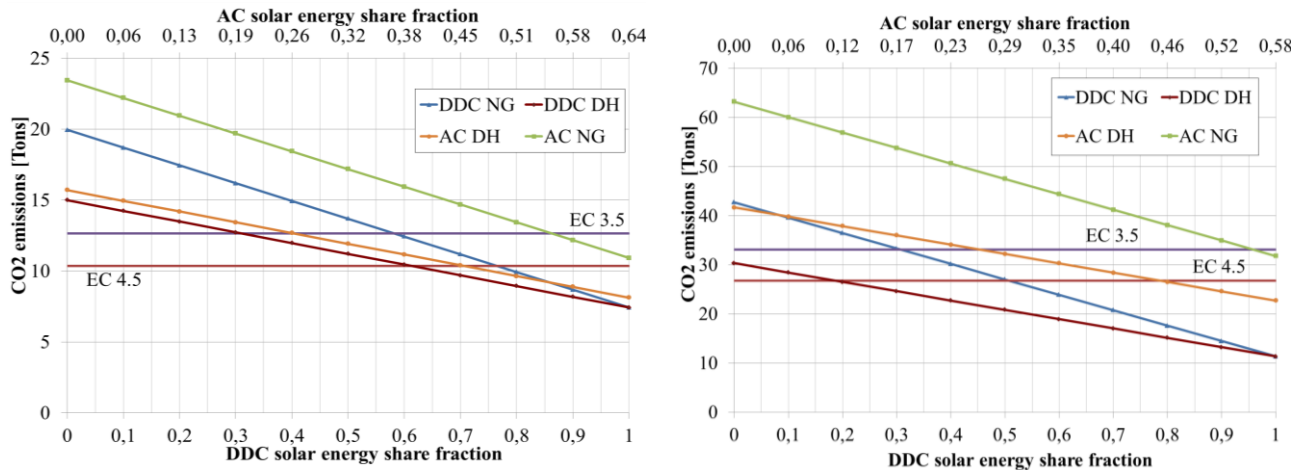
a) Copenhagen (seasonal  $Q_{reg,DDC}=55,5$  MWh)      b) Venice (seasonal  $Q_{reg,DDC}=137,9$  MWh)

Fig. 8. Energy costs as functions of the solar energy share fractions.

The energy costs in Venice are higher than in Copenhagen, reflecting higher energy consumptions. DH makes thermally driven systems very attractive. In Copenhagen the DDC system is more convenient than the ECs for  $f_{solar}$  higher than 0.1-0.5 with DH and 0.6-0.78 with NG, whereas AC is slightly more convenient than the DDC system for any  $f_{solar}$  with DH and results to be the most expensive system with NG. In Venice the DDC system is more convenient than the ECs for any  $f_{solar}$  with DH and for  $f_{solar}$  higher than 0.32-0.52 with NG. The AC is never more convenient than the DDC system.

### 3.2. CO<sub>2</sub> emissions

The same energy production technologies used in the energy cost analysis are considered, whose CO<sub>2</sub> emission data are taken from Danish statistics [20]: electricity 567 kg<sub>CO<sub>2</sub></sub>/MWh, NG 215 kg<sub>CO<sub>2</sub></sub>/MWh<sub>fuel</sub>, DH 137 kg<sub>CO<sub>2</sub></sub>/MWh. The resulting CO<sub>2</sub> emissions are reported in Fig. 9.



a) Copenhagen (seasonal  $Q_{reg,DDC}=55,5$  MWh)      b) Venice (seasonal  $Q_{reg,DDC}=137,9$  MWh)

Fig. 9. CO<sub>2</sub> emissions as functions of the solar energy share fractions.

The emissions in Venice are higher than in Copenhagen. The DDC system has relative low emissions in Venice, particularly with DH: already for a null  $f_{solar}$  its CO<sub>2</sub> emissions are lower than for the EC3.5, and always lower than the AC also considering NG. In Copenhagen the DDC

system with DH emits less than ECs for  $f_{solar}$  in the range of 0.3-0.6, while it always emits less than the corresponding AC.

## 4. Discussion

The energy analysis shows that for increasing latent loads on the systems, i.e. comparing Copenhagen and Venice, all systems have decreased performances but to different extents: the DDC system lowers its  $COP_t$  of approximately 37%, while chiller-based systems lower their  $COP_{t,AC}$  and  $COP_{e,4.5}$  of approximately 44%. This demonstrates that the DDC system is more efficient handling higher latent loads, in accordance to what reported in [4] for DEC systems in general.

The system comparison is based on the assumption that the supply airflow is constituted by 68% of air exhausted from the conditioned space. However, only the DW has an air cleaning potential. Lower recirculation rates of exhausted air in the chiller-based systems have to be used to obtain the same supply air quality, decreasing their performances.

The number of DPCs required to cover the sensible load (8 in Copenhagen and 12 in Venice) is higher than the minimum number of DPCs required to process the whole airflow. The difference is due to limited DPC performances. The DPCs are regulated by varying the airflow rate per DPC, since  $f_{rec}$  is set to 30%, maximizing the DPC net cooling capacity. The corresponding high number of DPCs increases investment costs, space requirements (the volume occupied by the considered DPC is  $1.3 \text{ m}^3$ ) and electricity consumption for the auxiliaries. A solution is to dehumidify the air to lower humidity ratios than what required for covering the latent load in the conditioned space. In fact, as shown in Fig. 5, the supply temperature is sensitive to the humidity ratio of the inlet primary airstream. This solution implies higher regeneration energy consumptions: its convenience depends on the availability of a cheap and clean heat source.

The electricity consumption for auxiliaries is higher for the DDC system than for the considered chiller-based systems. This is mainly due to the higher process flow rates, due to recirculation in the DPCs, and to the higher number of components. Electricity consumption can be reduced by removing the HRU. This would cause higher inlet temperatures to the DPCs and increased regeneration energy consumptions. Alternatively, the HRU can be unbalanced to reduce the fan power consumption.

The energy cost analysis and environmental impact of the systems are strongly dependent on the energy prices and emission data. The results represent the Danish scenario but they are likely to change in other countries. The Danish scenario is characterised by a price ratio between electricity and heat of 2.6 (electricity/NG) and of 5.6 (electricity/DH), and the  $\text{CO}_2$  emissions from electricity production are affected by the share of renewables and cogeneration plants.

The DDC system consumes water to cool the process air. The amount of water consumed in Copenhagen is almost tripled in Venice, because of the increased temperature at the DPC inlet conditions due to higher levels of dehumidification in the DW. However the processing of water to avoid formation of lime in the DPCs does not influence much the seasonal energy cost. It is estimated that water requires to be softened only if its pH is above 6.

## 5. Conclusion

The designed DDC system includes a specific DW made of silica gel, a generic HRU, specific DPCs, and it requires low grade heat sources. The DDC system is simulated to cover the sensible and latent loads of a specified supermarket from May to September in two different climates: temperate in Copenhagen and Mediterranean in Venice. Alternative systems based on electric and absorption chillers are also simulated and compared to the DDC system in terms of energy consumption, energy costs and  $\text{CO}_2$  emissions using data from the Danish scenario. The analysis shows that the DDC system can perform better than electric chiller-based systems if cheap and clean heat sources are available (e.g. solar energy or waste heat). Depending on the considered conventional heat sources and electric chiller COP, the DDC system is found to be competitive in

terms of energy costs for solar energy share fractions in the range of 10-78% in Copenhagen and 0-52% in Venice. Considering the CO<sub>2</sub> emissions, the ranges are 30-75% and 0-50% respectively. It can be concluded that the DDC system is a very convenient solution for the Mediterranean climate, while for the temperate climate its convenience is strongly dependent on the available heat source. Increasing sensible and especially latent loads make the regeneration energy consumption of absorption chillers increasing more than for the DDC system, while the electricity consumption for auxiliaries for the DDC system is higher. For this reason the DDC system is almost always more convenient than absorption chillers. The challenge for the DDC system is to reduce the high number of commercial-size DPC units required for covering the cooling load: 8 in Copenhagen and 12 in Venice. Optimized DPC size and control strategy can decrease the required number of DPCs. It is also assessed that reaching lower dew points after dehumidification would reduce the number of DPCs in the system.

## Appendix A – DPC model formulation

The DPC model is based on the following assumptions:

- The cooler is not exchanging heat with the surroundings.
- The air flows are evenly distributed among the channels.
- Heat conduction in the flow direction is neglected.
- Heat transfer in the vertical direction is neglected.
- The water distribution on top of the cooler is homogeneous.
- The vertical water distribution is homogeneous.
- The hygroscopic foils adhere to the plates perfectly.
- The hygroscopic foils are modeled as layers of water with negligible thermal resistance.

Under these assumptions, the smallest constitutive unit of the DPC is modeled, including half of a primary channel, half of a secondary channel, the hygroscopic layer and plate in between, along the whole DPC length. This unit is further discretized into smaller control volumes (CVs) along the DPC length. The discretized geometry is shown in Fig. 10.

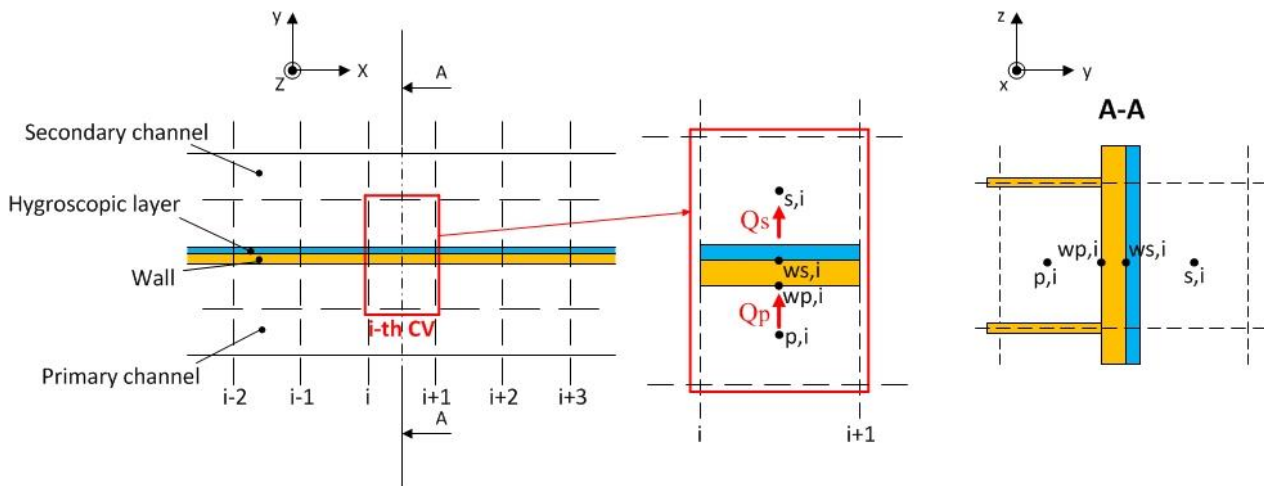


Fig. 10. Discretization of the geometry.

The governing equations for heat and mass transfer are discretized according to Fig. 3. The mass balances ensure conservation of the dry air mass flows in both sides and water vapor in the primary side, while in the secondary side also the evaporating water flow is accounted in the balance.

In the primary side, the energy balance for the generic  $i^{\text{th}}$  control volume is expressed as:

$$\dot{m}_{a,p} \cdot (I_{p,i+1} - I_{p,i}) - \dot{Q}_{p,i} = 0 \quad (1)$$

Where  $\dot{Q}_{p,i}$  is the sensible heat flux in [W] leaving the primary airstream,  $\dot{m}_{a,p}$  is the primary mass flow of dry air in [kg<sub>a</sub>/s] and  $I_{p,i}$  is the specific enthalpy in [J/kg<sub>a</sub>]. The sensible heat flux is determined by:

$$\dot{Q}_{p,i} = \bar{h}_{p,i} \cdot A_{p,i} \cdot (\bar{T}_{p,i} - \bar{T}_{wp,i}) \quad (2)$$

$\bar{T}_{p,i}$  and  $\bar{T}_{wp,i}$  are the primary airstream and wall temperatures in [°C], respectively. The bars indicate quantities referring to cell centered positions. The heat transfer coefficient  $\bar{h}_{p,i}$  [W/m<sup>2</sup>K] is computed using the built-in correlation in EES for duct flow. This correlation incorporates laminar, transition and turbulent flow; however, only laminar flow occurs for the whole range of conditions in this study. The upper and lower walls of the primary ducts are considered as fins, thus the primary side area  $A_{p,i}$  [m<sup>2</sup>] is corrected using the fin efficiency.

The thermal resistance of the wall  $R_{w,i}$  in [K/W] is taken into account to compute the wall temperature in the secondary side  $\bar{T}_{ws,i}$ :

$$\dot{Q}_{p,i} = \frac{\bar{T}_{wp,i} - \bar{T}_{ws,i}}{R_{w,i}} \quad (3)$$

The hygroscopic foil is modeled as a layer of water. During steady state operation, some of this water evaporates and the corresponding water vapor  $\dot{m}_{e,i}$  [kg/s] flows into the secondary airstream. The water content of the foils is maintained by the flow through the nozzles. In addition, the thermal resistance of the layer is considered negligible. The energy balance in the layer is:

$$\dot{Q}_{p,i} = \dot{Q}_{s,i} + \dot{m}_{e,i} \cdot c_{p,water} \cdot (\bar{T}_{ws,i} - T_{water,i}) = \dot{Q}_{s,i} + \dot{Q}_{water} \quad (4)$$

The second term on the right hand side accounts for bringing the added water in equilibrium with the adjacent wall. The remaining heat flux  $\dot{Q}_{s,i}$  flows to the secondary side.

In the secondary side, the energy balance is expressed as:

$$\dot{m}_{a,s} \cdot (I_{s,i+1} - I_{s,i}) + \dot{Q}_{s,i} = 0 \quad (5)$$

$\dot{m}_{a,s}$  is proportional to  $\dot{m}_{a,p}$  by defining the recirculation fraction  $f_{rec}$  as the ratio between the secondary and primary air volume flow rates.  $\dot{Q}_{s,i}$  is computed as the sum of the sensible and latent heat flows:

$$\dot{Q}_{s,i} = \dot{Q}_{s,sens,i} + \dot{Q}_{s,lat,i} \quad (6)$$

$$\dot{Q}_{s,sens,i} = \bar{h}_{s,i} \cdot A_{s,i} \cdot (\bar{T}_{ws,i} - \bar{T}_{s,i}) \quad (7)$$

$$\dot{Q}_{s,lat,i} = r \cdot \dot{m}_{e,i} = r \cdot \bar{\sigma}_i \cdot A_{s,i} \cdot (\omega_{ws,i} - \omega_{s,i}) \quad (8)$$

The heat transfer coefficient  $\bar{h}_{s,i}$  is computed using the built-in correlation in EES for duct flow. The heat and mass transfer analogy is used to compute the mass transfer conductance  $\bar{\sigma}_i$  in [kg/m<sup>2</sup>s]. Due to the simplifications of the model the mass transfer capacity of the secondary side may be sufficient to reach over-saturated conditions. However, this is not a realistic operating condition. In this it the secondary airstream is limited to saturated conditions and the amount of evaporating water is adjusted accordingly.

Along the DPC entrance, where water is not sprayed on top (see Fig. 3), an area effectiveness coefficient of 0.1 is applied. Such a low value is motivated by the fact that the airstreams have a cross flow arrangement, and the absence of the spraying box on top leads to non-optimal wetting of the hygroscopic foils.

Pressure losses are estimated for both the primary and secondary airstreams, considering three contributions: pressure drop due to initial acceleration, pressure drop due to internal friction, and pressure gain due to final deceleration of the airstream. The friction factor is computed using built-in correlations in EES.

## References

- [1] European Commission. Climate Action. Policies. Climate and energy package – Available at: <[http://ec.europa.eu/clima/policies/package/index\\_en.htm](http://ec.europa.eu/clima/policies/package/index_en.htm)> [accessed 5.3.2013].
- [2] Choudhury B., Saha B.B., Chatterjee P.K., Sarkar J.P., An overview of developments in adsorption refrigeration systems towards a sustainable way of cooling. *Applied Energy* 2013;104(0):554-567.
- [3] Awbi H., *Ventilation of buildings*. Spon Press; 2003.
- [4] Daou K., Wang R., Xia Z., Desiccant cooling air conditioning: A review. *Renewable and Sustainable Energy Reviews* 2006;10(2):55-77.
- [5] ASHRAE Handbook - Fundamentals. American Society of Heating, Refrigerating and Air-Conditioning Engineers; 2009.
- [6] ASHRAE Handbook – HVAC Systems and Equipment. American Society of Heating, Refrigerating and Air-Conditioning Engineers; 2008.
- [7] La D., Dai Y.J., Li Y., Wang R.Z., Ge T.S., Technical development of rotary desiccant dehumidification and air conditioning: A review. *Renewable and Sustainable Energy Reviews* 2010;14(1):130-147.
- [8] Ling J., Kuwabarab O., Hwang Y., Radermacher R., Enhancement options for separate sensible and latent cooling air-conditioning systems. *Internal Journal of Refrigeration* 2013;36(1):45-57.
- [9] Uges P.G:H., Technical workshop: a closer look at evaporative adiabatic wet bulb cooling and diabatic dew-point cooling, using water (R718) as refrigerant. GL 2010: Proceedings of the 9th IIR Gustav Lorentzen Conference, 2010; Sidney, Australia.
- [10] Bellemo L., New desiccant cooling system using the regenerative indirect evaporative process [master thesis]. Kgs. Lyngby, Denmark: department of Mechanical Engineering, Technical University of Denmark; 2011.
- [11] Jain S., Dhar P., Kaushik S., Evaluation of solid-desiccant-based evaporative cooling cycles for typical hot and humid. *Internal Journal of Refrigeration* 1995;18(5):287-296.
- [12] Goldsworthy M., White S., Optimisation of a desiccant cooling system design with indirect evaporative cooler. *Internal Journal of Refrigeration* 2011;34(1):148-158.
- [13] Zhang G., Zhang Y.F., Fang L., Theoretical study of simultaneous water and VOCs adsorption and desorption in a silica gel rotor. *Indoor Air* 2008;18(1):37-43.
- [14] Ge T.S., Li Y., Wang R.Z., Dai Y.J., A review of the mathematical models for predicting rotary desiccant wheel. *Renewable and Sustainable Energy Reviews* 2008;12(6):1485-1528.
- [15] NovelAire Technologies – Available at: <<http://www.novelaire.com>> [accessed 5.3.2013].
- [16] Statiqcooling – Available at: <<http://www.statiqcooling.nl>> [accessed 5.3.2013].
- [17] Janssen M., Uges P.G:H., Parameters affecting the performance of a dewpoint cooler consisting of a counter flow heat exchanger using water as refrigerant. GL 2010: Proceedings of the 9th IIR Gustav Lorentzen Conference, 2010; Sidney, Australia.
- [18] Bellemo L., Elmegaard B., Reinholdt L.O., Kærn M.R., Modeling of a regenerative indirect evaporative cooler for a desiccant cooling system. To be published in the proceedings of the 4<sup>th</sup> IIR Conference on Thermophysical Properties and Transfer Processes of Refrigerants; 2013 June 16-19; Delft, Holland.
- [19] Siemens. Downloads. Refrigeration Technology. – Available at: <[http://www.hqs.sbt.siemens.com/gip/general/dlc/data/assets/hq/Refrigeration-technology\\_8359\\_hq-en.pdf](http://www.hqs.sbt.siemens.com/gip/general/dlc/data/assets/hq/Refrigeration-technology_8359_hq-en.pdf)> [accessed 5.3.2013].
- [20] Danish Energy Agency. Publications. Energy Statistics 2009. Available at: <<http://large.stanford.edu/courses/2010/ph240/smillie1/docs/energy-dk-2009.pdf>> [accessed 5.3.2013].